Supplementary data

Dual Contrast Agents for Fluorescence and Photoacoustic Imaging: Evaluation in a Murine Model of Prostate Cancer

Wojciech G. Lesniak[a*], Yixuan Wu[b,c*], Jeeun Kang[a,c], Srikanth Boinapally[a], Sangeeta Ray Banerjee[a], Ala Lisok[a], Anna Jablonska[a,d], Emad M. Boctor[a,b,c,e**] and Martin G. Pomper[a**]

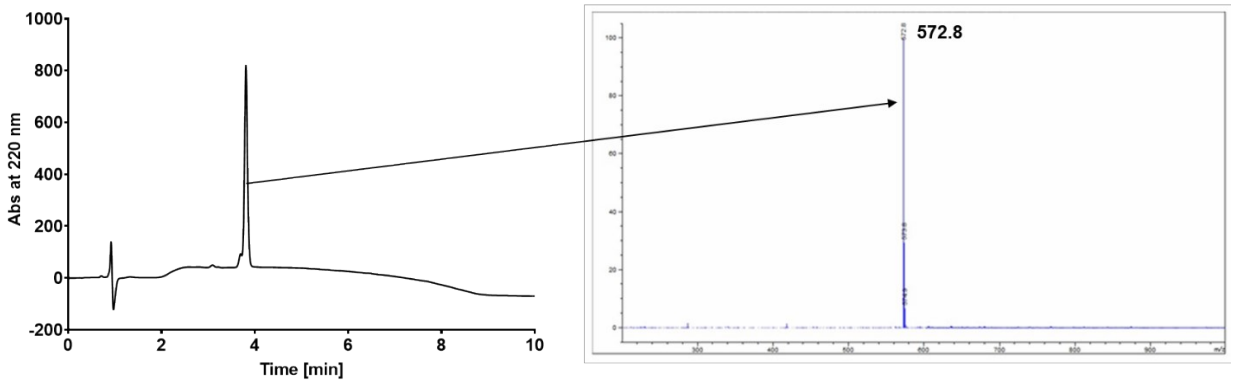

Figure S1. RP-HPLC chromatogram and ESI-MS spectrum indicates high purity of NHS-SA-KEU.

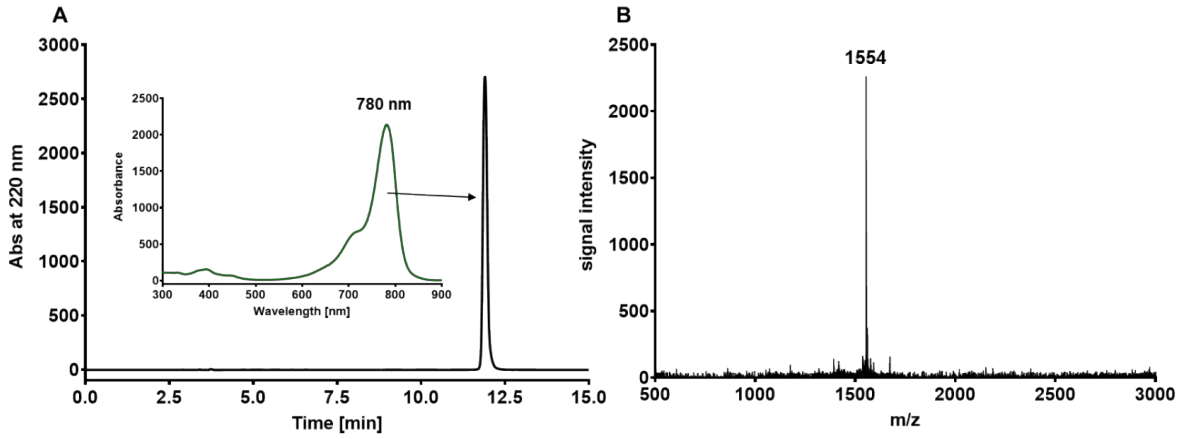

Figure S2. A - RP-HPLC chromatogram of C7.5-K-SA-KEU (conjugate **I**) with the UV-Vis spectrum recorded under the peak (insert), indicating covalent attachment of Cy7.5 to the K-SA- KEU moiety; **B -** MALDI-TOF spectrum of conjugate **I**, confirming its identity with molecular mass of 1554 Da.

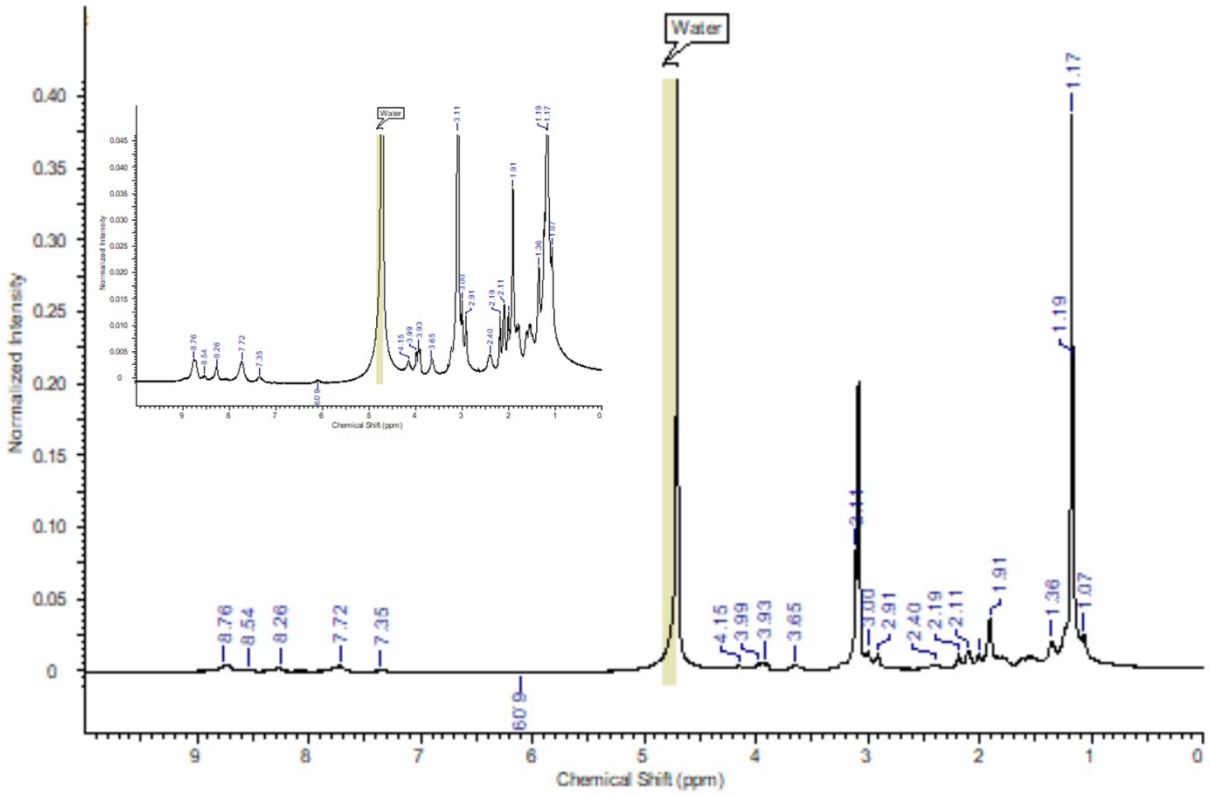

Figure S3. ^{1}H NMR of conjugate **I** (Cy7.5-lysine-subaric acid-lysine-glutamate-urea - Cy7.5-K-SA-KEU), showing the presence of Cy7.5 in the sample due to of the signals in the aromatic range between 7 and 9 ppm. However, due to large number of protons and broad overwrapping signals assignment of peaks related to individual protons is not feasible.

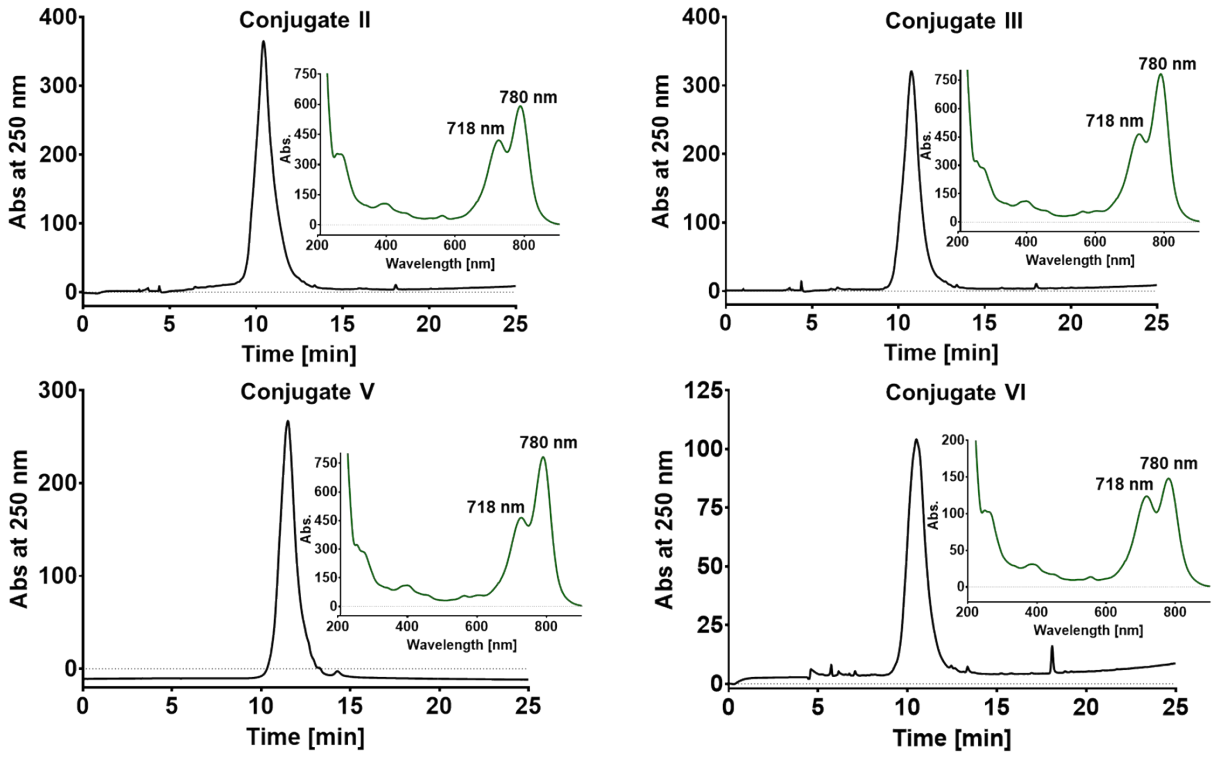

Figure S4. A - RP-HPLC chromatogram of dendrimer conjugates conjugate **II**, **III V** and **VI** with the UV-Vis spectrum recorded under the peak (insert), showing their purity and covalent attachment of Cy7.5.

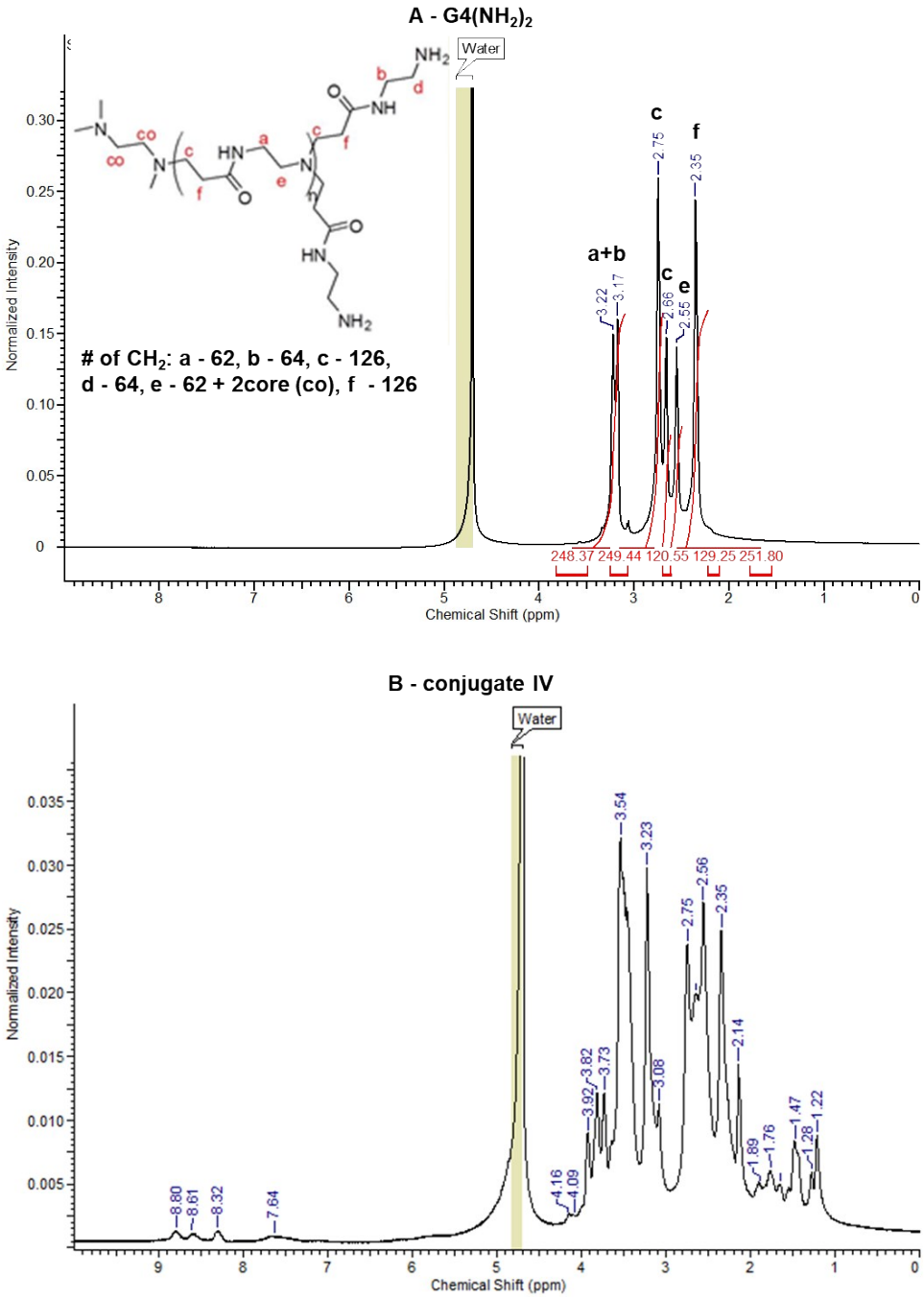

Figure S 5. **^{1}H NMR A** - spectrum of generation 4 ethylenediamine core poly(amidoamine) dendrimer terminated with primary amines Insert - partial structure of dendrimer (n=3) with theoretical number of CH_2 groups. Integrals are in good agreement with the number of protons in each group of CH_2 moieties. **B** - spectrum of conjugate **IV** $[G4(Cy7.5)_6(SA\text{-}KEU)_9(Bdiol)_{53}]$ confirming conjugation of Cy7.5 with dendrimer due to presence of the signals in the aromatic range between 7 and 9 ppm. Assignment of other peaks and is not feasible because of broad and overlying signals related to dendrimer and conjugated moieties. Spectra were recorded using a 500 MHz Bruker spectrometer (Bruker Biosciences, Billerica, MA, USA) and D_2O as solvent.

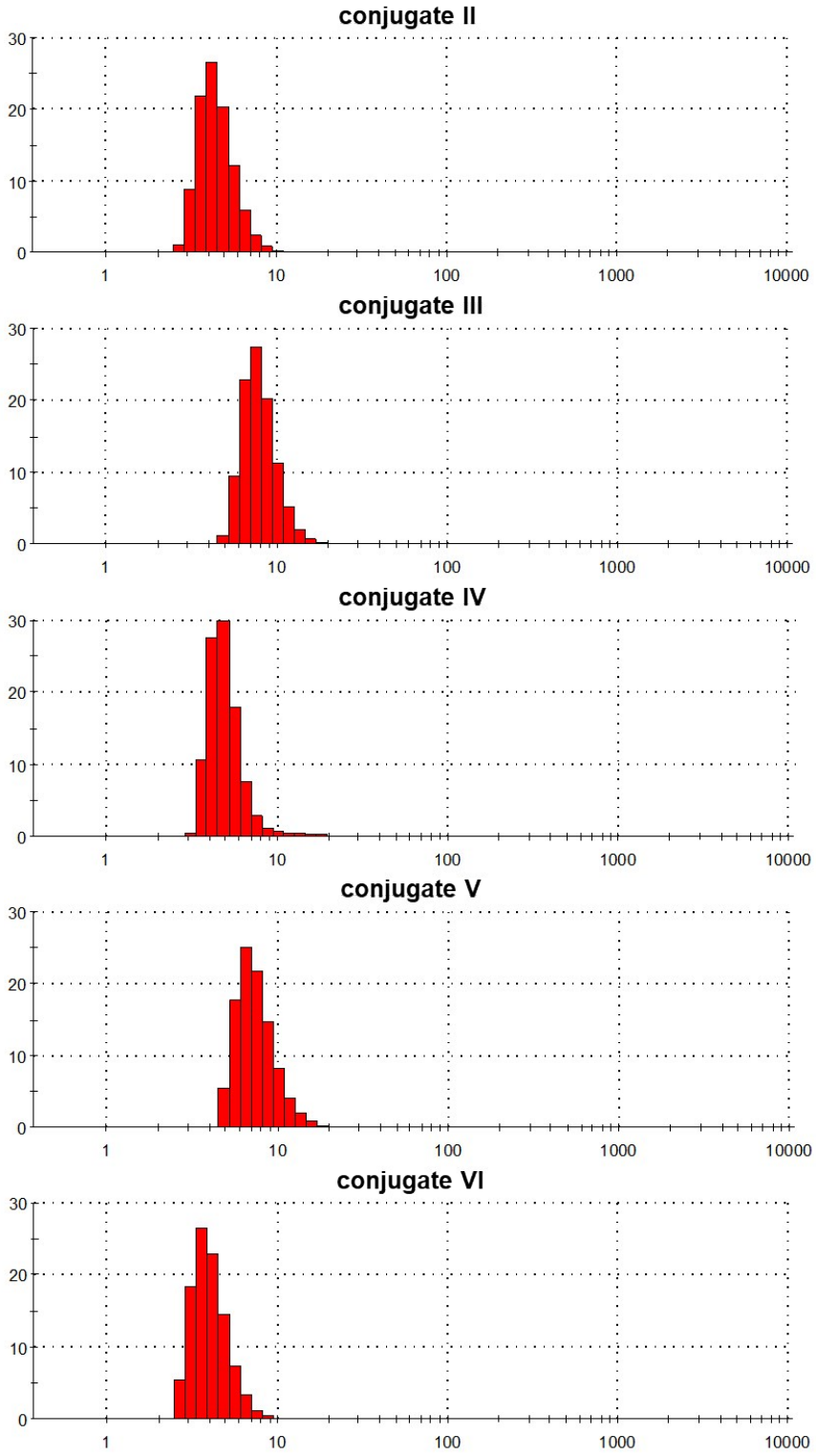

Figure S6. Dynamic light scattering. Representative of number weighted size distribution of dendrimer conjugates.

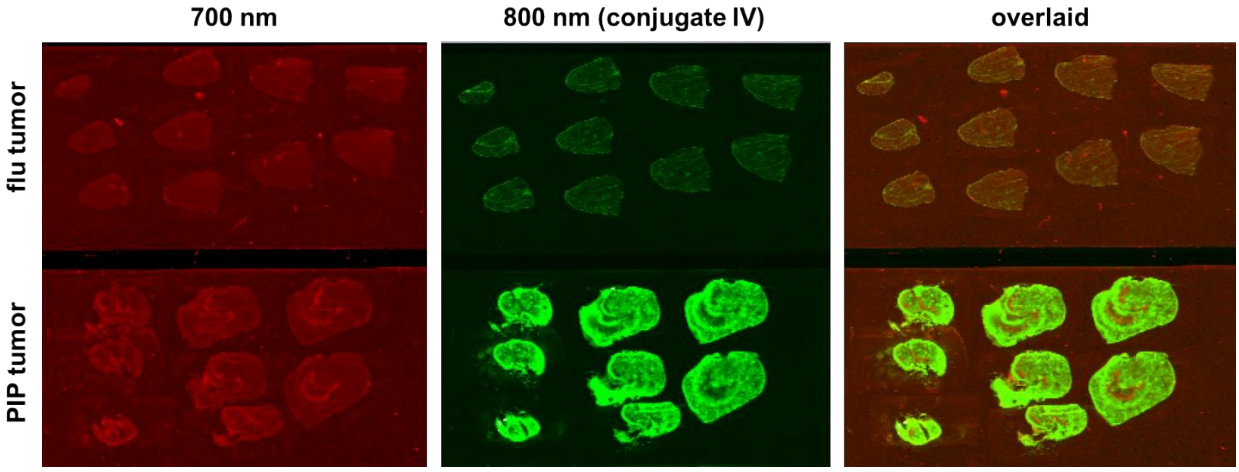

Figure S7. *Ex vivo* evaluation of conjugate **IV** uptake in $PSMA^{+}$ PC3 PIP and $PSMA^{-}$ PC3 tumors in specimen dissected 72 h after injection and scanned using a Li-Cor Odyssey infrared imaging system using 700 nm (excitation 685 and emission 730 nm, red) and 800 nm (excitation 785 and emission 830 nm green) channels, demonstrating its presence throughout entire tumor.

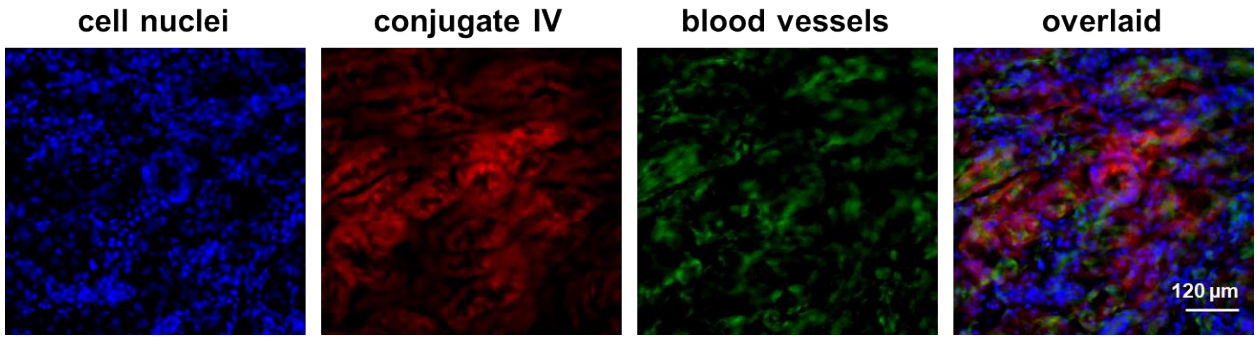

Figure S8. *Ex vivo* evaluation of conjugate **IV** uptake in kidneys showing its presence in proximal convoluted tubules.

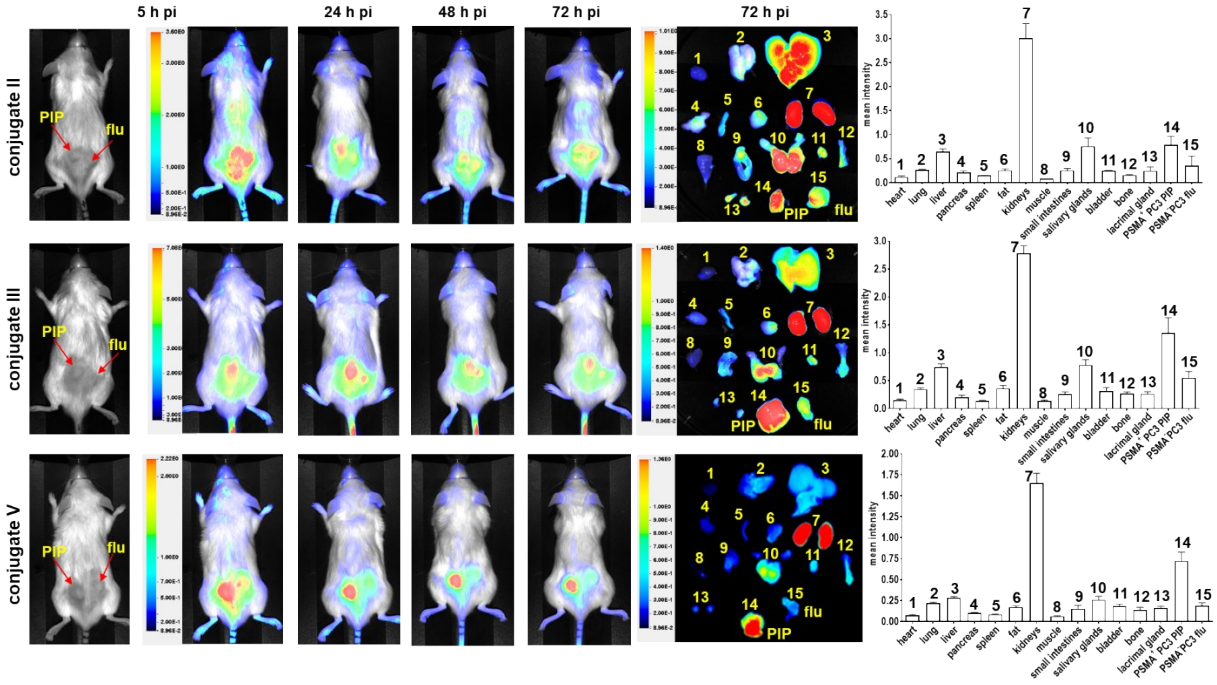

Figure S9. NIR FL imaging of conjugate II, III and V. NOD-SCID mice bearing subcutaneous PSMA^{+} PC3 PIP and PSMA^{-} PC3 flu in the lower back near left and right posterior flanks, respectively, were injected with given conjugate at dose equivalent to 22 nmol of Cy7.5 and images in the visible and NIR (excitation 785 and emission 820 nm) channels were acquired at 5, 24, 48 and 72 h after injection; corresponding images of *ex vivo* biodistribution and semi-quantitative analysis of fluorescence intensity (column numbers in the graph represent the tissue numbers, n=5). Data indicate preferential uptake of the conjugates in PSMA^{+} PC3 PIP tumors vs. PSMA^{-} PC3 flu tumors with their relatively high uptake in kidneys compared to conjugate **IV**.

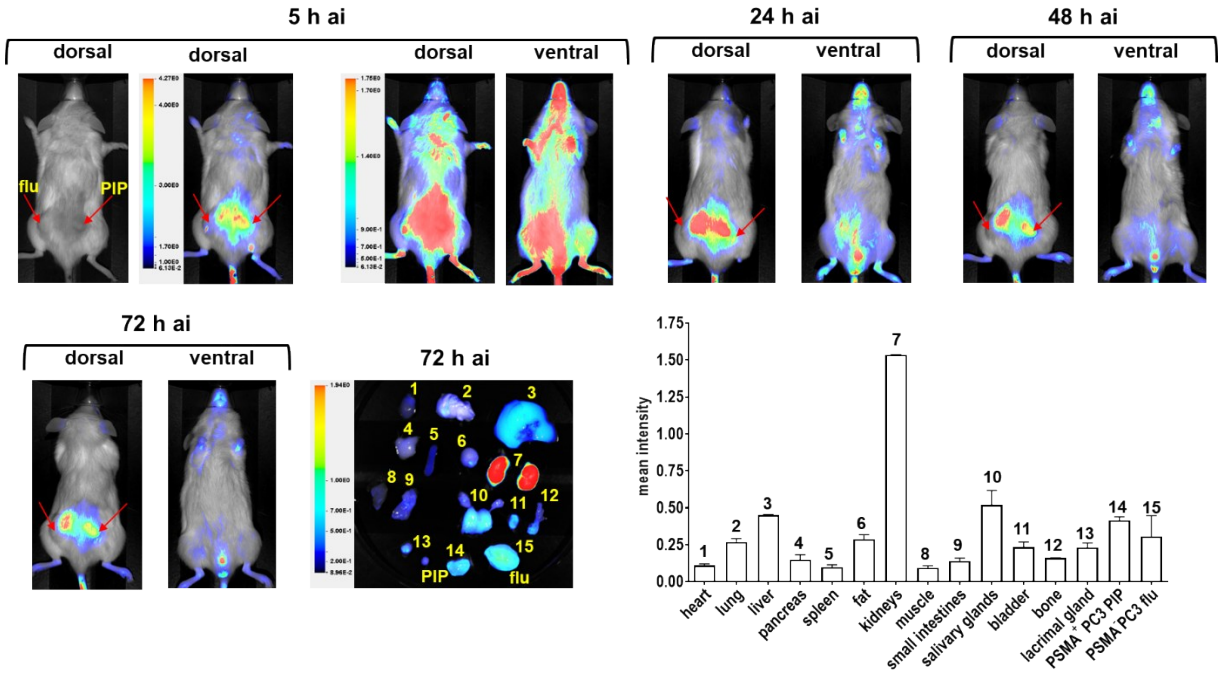

Figure S10. NIR FL imaging. Representative optical image of NOD-SCID mice bearing subcutaneous PSMA^{+} PC3 PIP and PSMA^{-} PC3 flu in the lower back near right and left posterior flanks, respectively (as indicated by arrows), injected with non-targeted control dendrimer conjugate **VI**. Images were acquired using visible and NIR (excitation 785 and emission 820 nm) channels. In contrast to PSMA-targeted dendrimer conjugates, control conjugate did not show preferential uptake in PSMA^{+} PC3 PIP tumors. Signal observed in the *in vivo* images was localized in kidneys as confirmed by *ex vivo* organs imaging.

Conjugate **I** (SRI-05-21, Cy7.5-K-SA-KEU) YC-27 (IR800CW-K-SA-KEU)

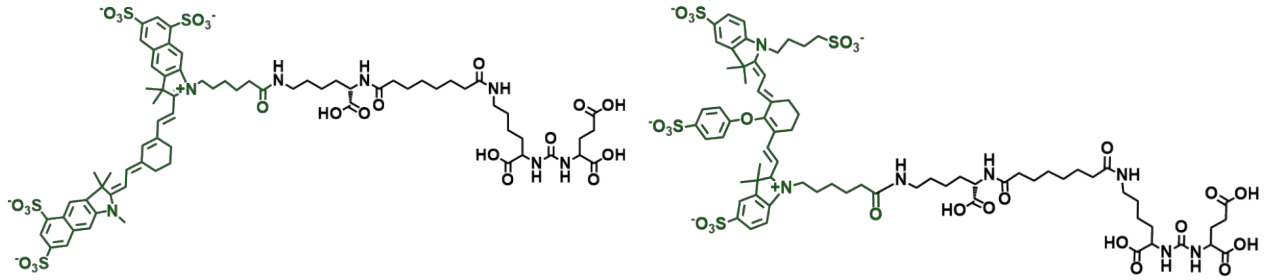

Figure S11. Structure of the conjugate **I** and YC-27.

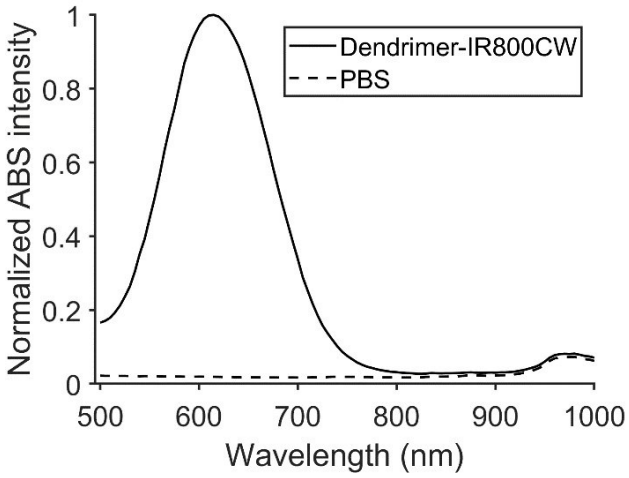

Figure S12. The spectrophotometry of PAMAM dendrimer-IR800CW conjugate was measured using the same system described in section NIR Spectrophotometry and Spectrofluorometry. Figure shows the optical absorbance of the conjugate in the range of 500 nm to 1000 nm in 5 nm interval, where the absorbance peaks at 610 nm then sharply decreases as the wavelength increases. In consequence, the absorbance of the conjugate cannot be well distinguished from the one of PBS from 700 nm to 900 nm, thus is not ideal for the NIR PA PC study on our PA system. Similar results were observed for the PAMAM dendrimer-IR800CW conjugates regardless number of the IR800CW dyes conjugated with dendrimer ranging from 2 to 6.